<u>Supporting information</u>

Zn(II)-Embedded Nanoporous Covalent Organic Frameworks for Catalytic Conversion of CO$_2$ under Solvent-Free Conditions

Najirul Haque[a], Surajit Biswas[a], Swarbhanu Ghosh[a], Arpita Hazra Chowdhury[a], Aslam Khan[b], and Sk Manirul Islam[a]*

[a] Department of Chemistry, University of Kalyani, Kalyani, Nadia, 741235, W.B., India.

[b] King Abdullah Institute for Nanotechnology, King Saud University, Riyadh, 11451, Saudi Arabia.

*Corresponding author; *E-mail: manir65@rediffmail.com*

Table of Contents

Materials

All chemicals were purchased from commercially available sources and used as received without further purification. Solvents were distilled and dried through standard methods before use.

Characterization Techniques

A D8 Advance SWAX diffractometer from Bruker-AXS utilizing a constant current (40 mA) and voltage (40 kV) was used to obtain the powder XRD pattern of the Zn@RIO-1 catalyst. The XRD machine was calibrated with silicon sample utilizing Ni-filtered Cu K$_\alpha$ radiation (λ=0.15406 nm). On a Perkin–Elmer FTIR 783 spectrophotometer the Fourier transform infrared (FTIR) spectra of the catalysts were recorded from 400 to 4000 cm^{-1} using KBr pellets. Using a Shimadzu, Japan, UV-2401PC doubled beam spectrophotometer with an integrating sphere attachment for solid based samples UV-Vis spectra was taken. Scanning electron microscope (SEM) (ZEISS EVO40, England) equipped with EDX facility was used to measure surface morphology of the Zn@RIO-1. BET surface area and porosity of these materials were estimated from the respective N_2 sorption isotherms at 77 K by using a Quantachrome Instruments Autosorb-1C surface area analyzer. The samples were activated at 403 K under high vacuum for 12 h before the N_2 adsorption−desorption analysis. The pore size distributions were estimated from these N_2 sorption isotherms using the nonlocal density functional theory (NLDFT) and carbon/slit pore model as reference. TEM images were recorded using FEI Tecnai G2 F20 X-TWIN TEM at an accelerating voltage of 200 kV. HR-TEM, 5 mg of the Zn@RIO-1 catalyst was dispersed into absolute EtOH under the application of sonication for 30 min, followed by the sample coating on a carbon coated copper TEM grid and dried in air. Using a Mettler Toledo TGA/DTA851 instrument

thermogravimetric analysis (TGA) was done. Optima 2100DV (Perkin Elmer) inductively coupled plasma atomic emission spectroscopy (ICP-AES) was used for measurement of silver amount present in the catalyst. All spectra were taken at 400 MHz for ^{1}H NMR. Using Bruker DPX-400 in $CDCl_3$ instrument with TMS as internal standard the products was confirmed by ^{1}H spectroscopy.

Experimental

Synthesis of 1,3,5-triformylphloroglucinol (TFPG)

TFPG has been produced by using our previously reported procedures.[1,2] In brief, to a combination of 3 g of dried phloroglucinol and 7.4 g HMT (hexamethylenetetramine), trifluoroacetic acid (45 mL) was added. The addition of trifluoroacetic acid was conducted carefully in ice bath. Then the temperature of the mixture was slowly increased to RT. The reaction mixture was then allowed to reflux at 100 ˚C for 2.5 hour under N_2 atmosphere. Next, 3 M hydrochloric acid was added to it drop by drop and was further refluxed for another 1 hour. Finally, the solution was allowed to cool to RT and filtered the solution through celite bed. Obtained filtrate was extracted with DCM (4 times) and dried over anhydrous Na_2SO_4. The extract was then concentrated to yield yellow colored solid. By using hot ethanol, obtained crude product was purified to yield the desired product and ^{1}HNMR in ^{1}H NMR ($CDCl_3$, 400 MHz) δ (ppm) 10.165 (s, -CHO), 14.1381 (s, -OH).

Synthetic procedure of RIO-1 covalent organic framework (3D-COF) material

Synthesis of catalyst RIO-1 porous polymeric material was carried out by reacting triformyl phloroglucinol (TFPG) (200 mg) with tetrakis-4-amino phenylmethane (TAP) (150 mg) in presence of (7.5 mmol) 1.46 gm p-toluenesulfonic acid (PTSA). At first PTSA and orange colored TAP were mixed homogeneously in a mortar-pestle and the mixture was grinded uniformly for 12-15 minutes to retrieve a gluey pale yellowish colored material. TFPG (100mg) was then added to this mixture and grinding was continued for another 15 minutes.

The material became yellowish orange in color. To make this mixture viscous, dropwise dough distilled water (100-200 μL) were added. The material, collected in Teflon-lined steel

autoclave was heated initially 60°C for 6h and increased to 90°C for another 9h in steady

condition. The developed material (RIO-1) was placed at room temperature for cooling down

and washed by N,N-dimethylacetamide (DMAc) for 4–5 times. Finally, acetone was used as

washing liquid to remove the residuals of starting materials. Orange-red coloured powder like

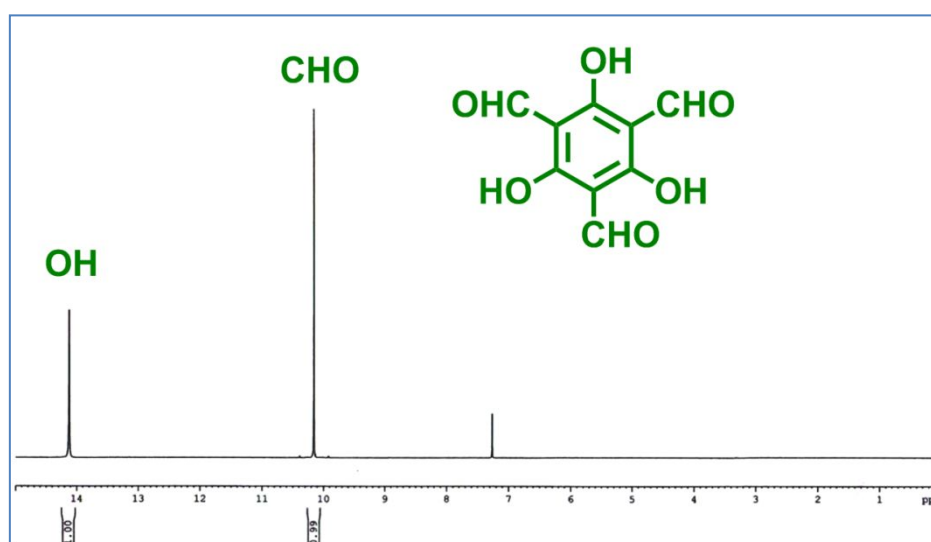RIO-1 COF was collected after kept under vacuum desiccation for 24h.

Figure S1: ^{1}H NMR of 1,3,5-triformylphloroglucinol (TFPG).

Catalytic α-alkylidene cyclic carbonate synthesis from propargyl alcohols

In a 25ml round bottom flask, 5 mmol of propargyl alcohol derivative, 5mmol 1,8-Diazabicyclo(5.4.0)undec-7-ene (DBU) and 10 mg of catalyst Zn@RIO-1were taken. The RB was attached with CO_2 balloon and the mixture was allowed to stir at room temperature for 10h. Thin layer chromatography (TLC) method was used to check the reaction progress. Upon completion of the reaction, the mixture was filtered to separate Zn@RIO-1, the filtrate was extracted with ethyl acetate and dried over sodium sulphate. The obtained product was purified by column chromatography and characterized with ^{1}HNMR spectroscopy.

Catalytic oxazolidiniones synthesis from propargyl alcohols and amines

5 mmol of propargyl alcohol was mixed with 5 mmol of amine in a 25 ml RB flask. 15 mg of Zn@RIO-1catalyst was added to this system. The RB was attached with CO_2 balloon and the mixture was allowed to stir at 80°C for 12 h. Reaction progress was monitored by TLC

method. Zn@RIO-1 was separated by filtration and the filtrate was extracted with ethyl acetate. The product was purified by column chromatography and characterized with ^{1}HNMR spectroscopy.
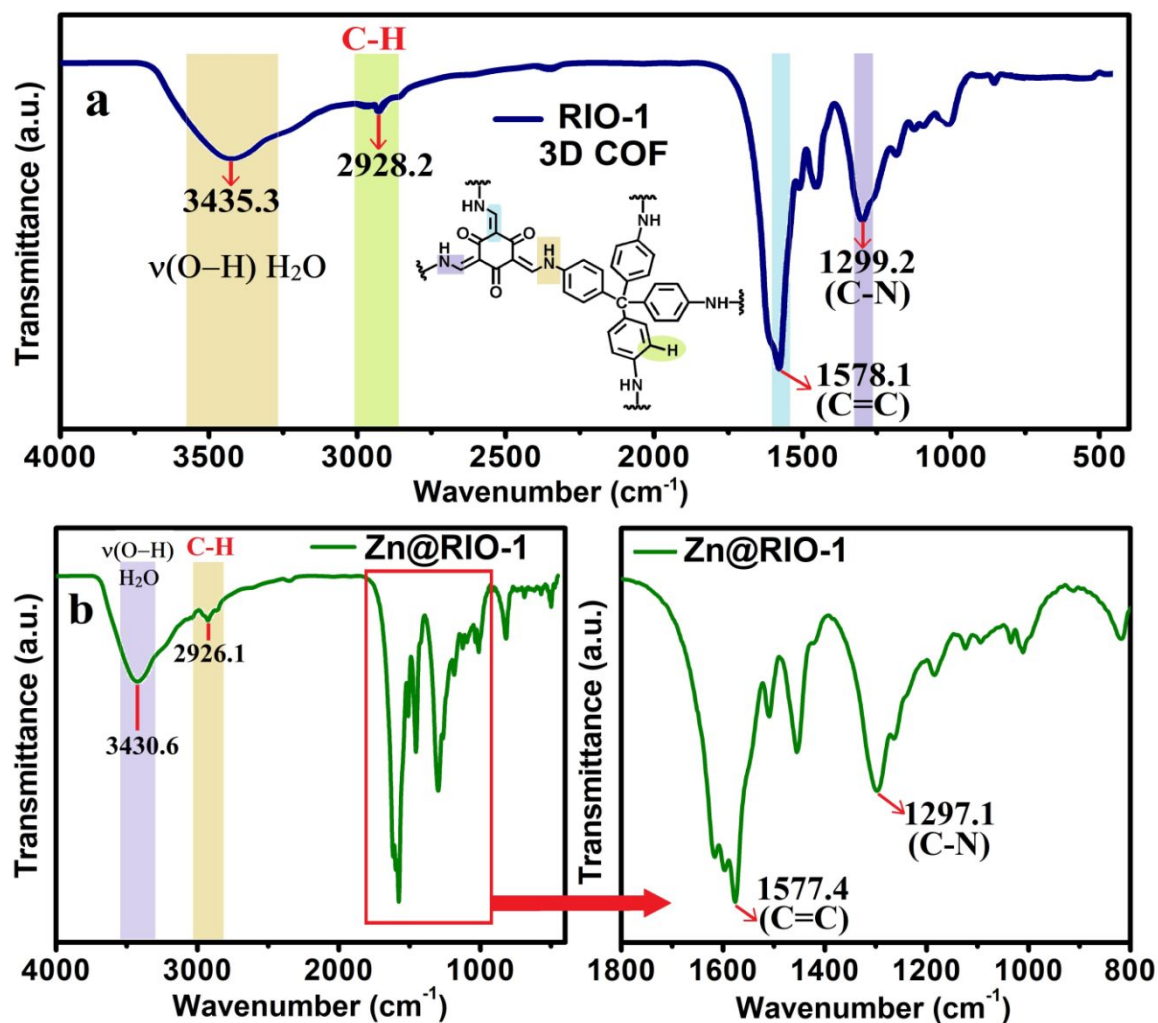

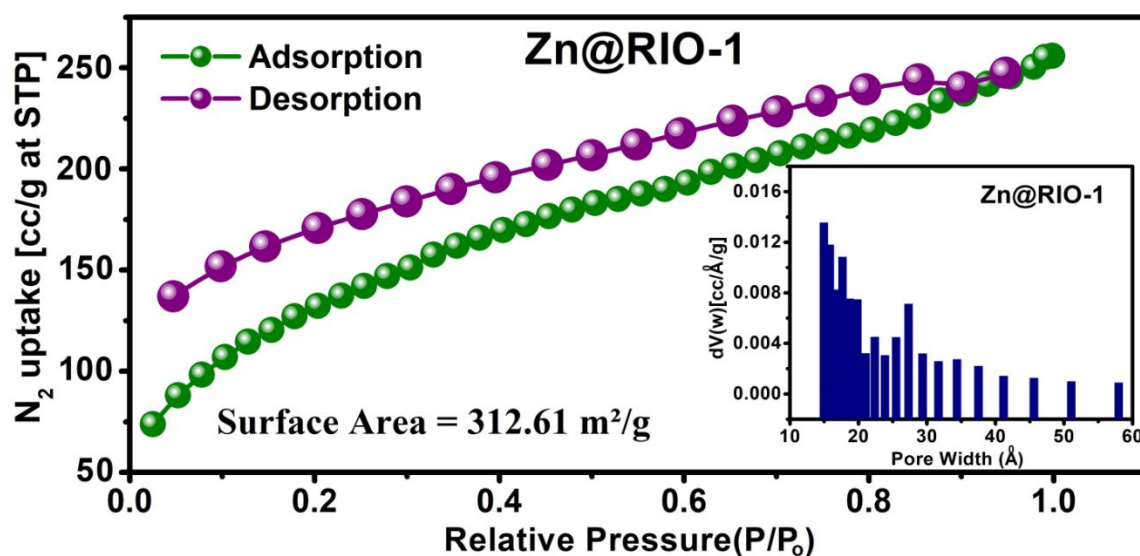**Figure S2.** FT-IR spectra of RIO-1 (a) and Zn@RIO-1 (b).

Figure S3. N_2 adsorption–desorption isotherm of Zn@RIO-1 material at a certain temperature (77 K). Pore size distribution is shown in the inset.

Our Catalyst Zn@RIO-1 displayed good BET surface area as compared to previously reported COF fabricated by Islam and co-workers.[3] from our laboratory and almost similar surface area to the 3D COF demonstrated by Li and co-workers.[4] The measured surface area retains the same as that of the reported COF published by Islam and Li. So, we can conclude that our developed 3D Zn anchored covalent organic framework corroborates well with these previous reports.
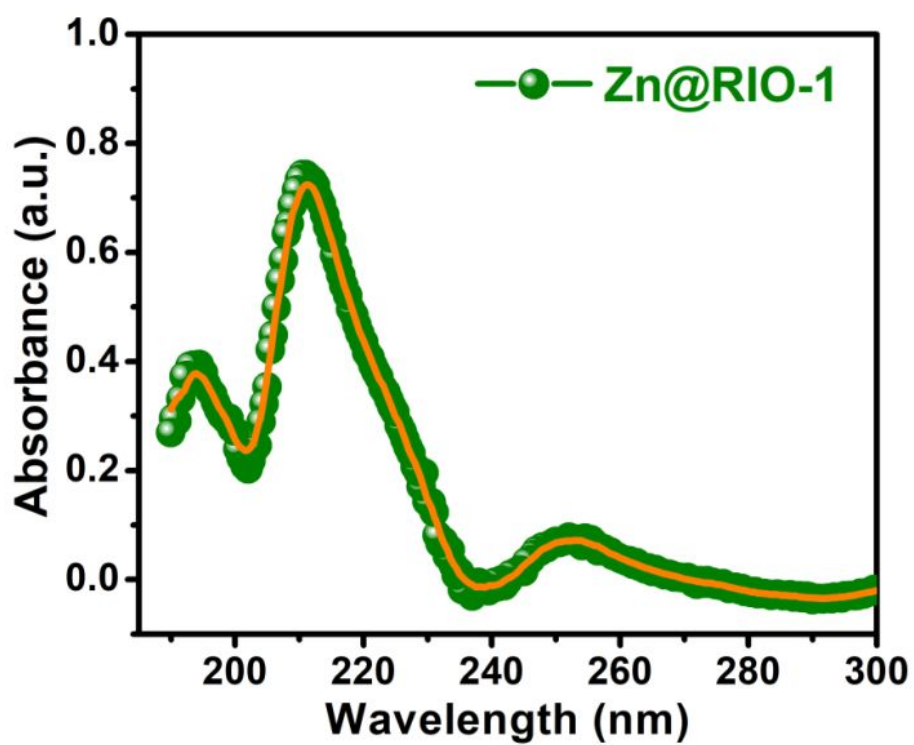
Figure S4. UV-Vis absorption spectrum of Zn@RIO-1 material.

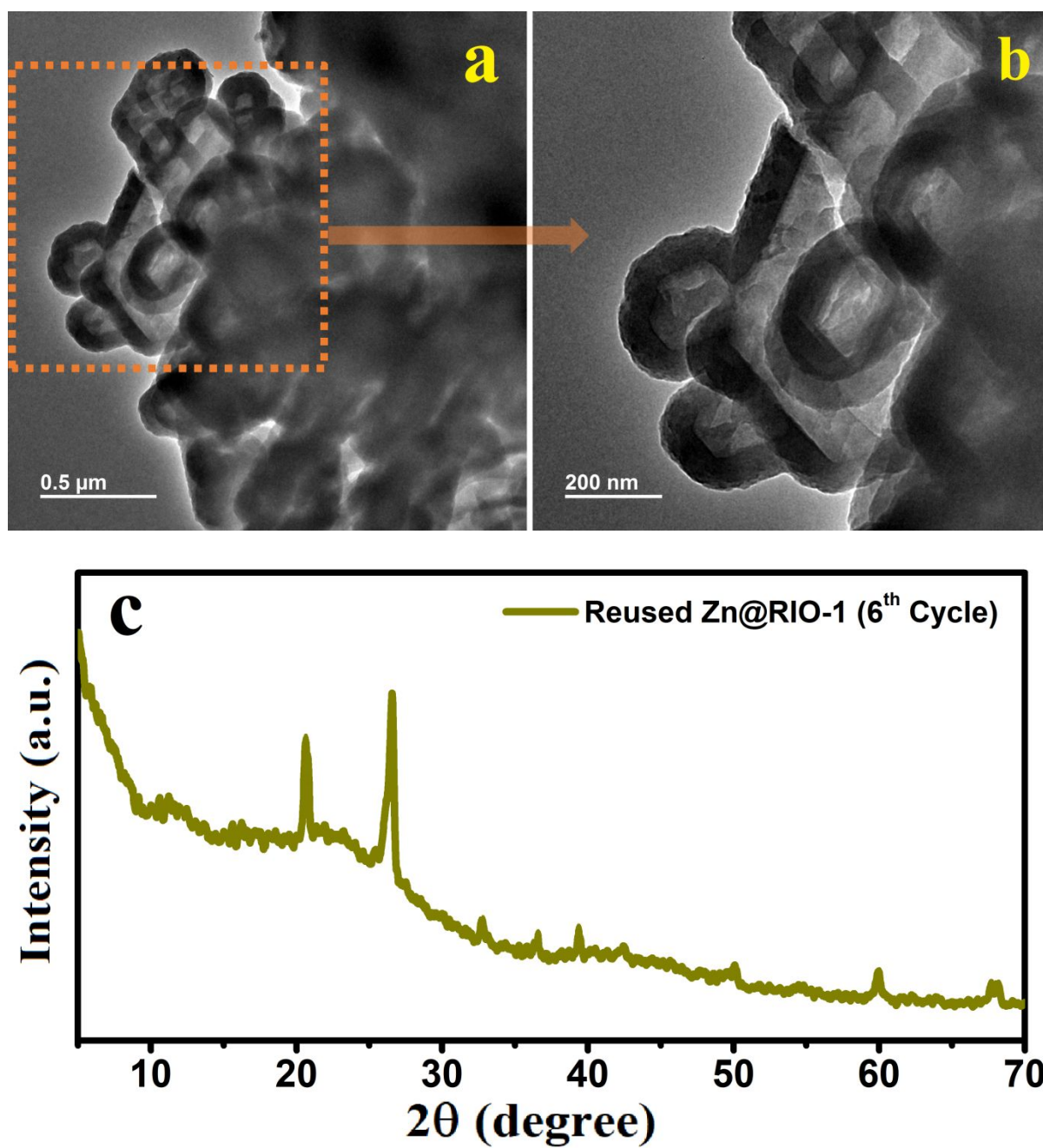*Characterization of reused Zn@RIO-1 catalyst*

Figure S5: TEM images of reused Zn@RIO-1 at different scales (a) 0.5 μm and (b) 200 nm, and (c) PXRD pattern after 6th run.
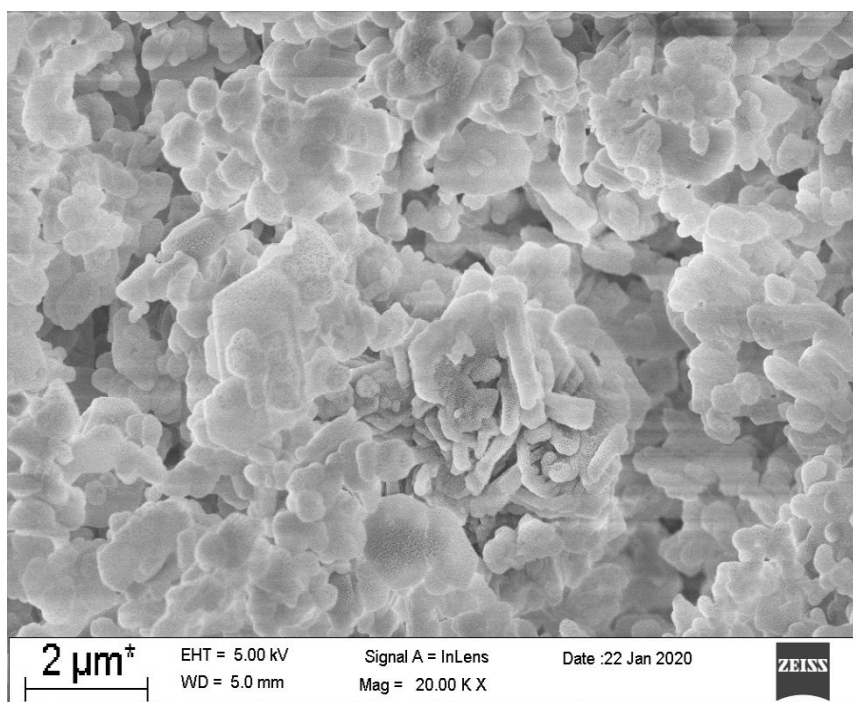
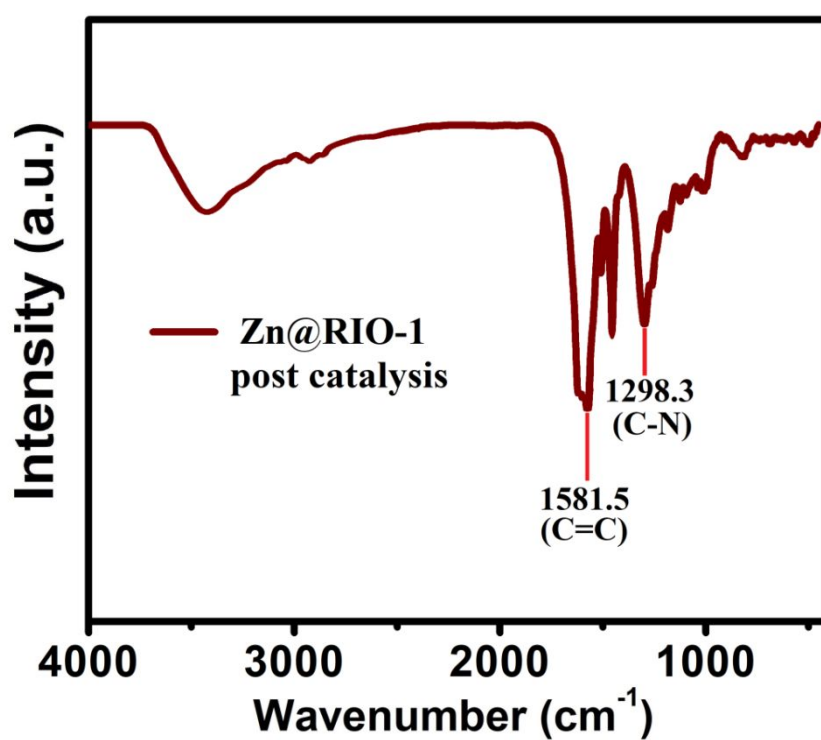**Figure S6:** FE-SEM picture of reused Zn@RIO-1 material after 6th run.

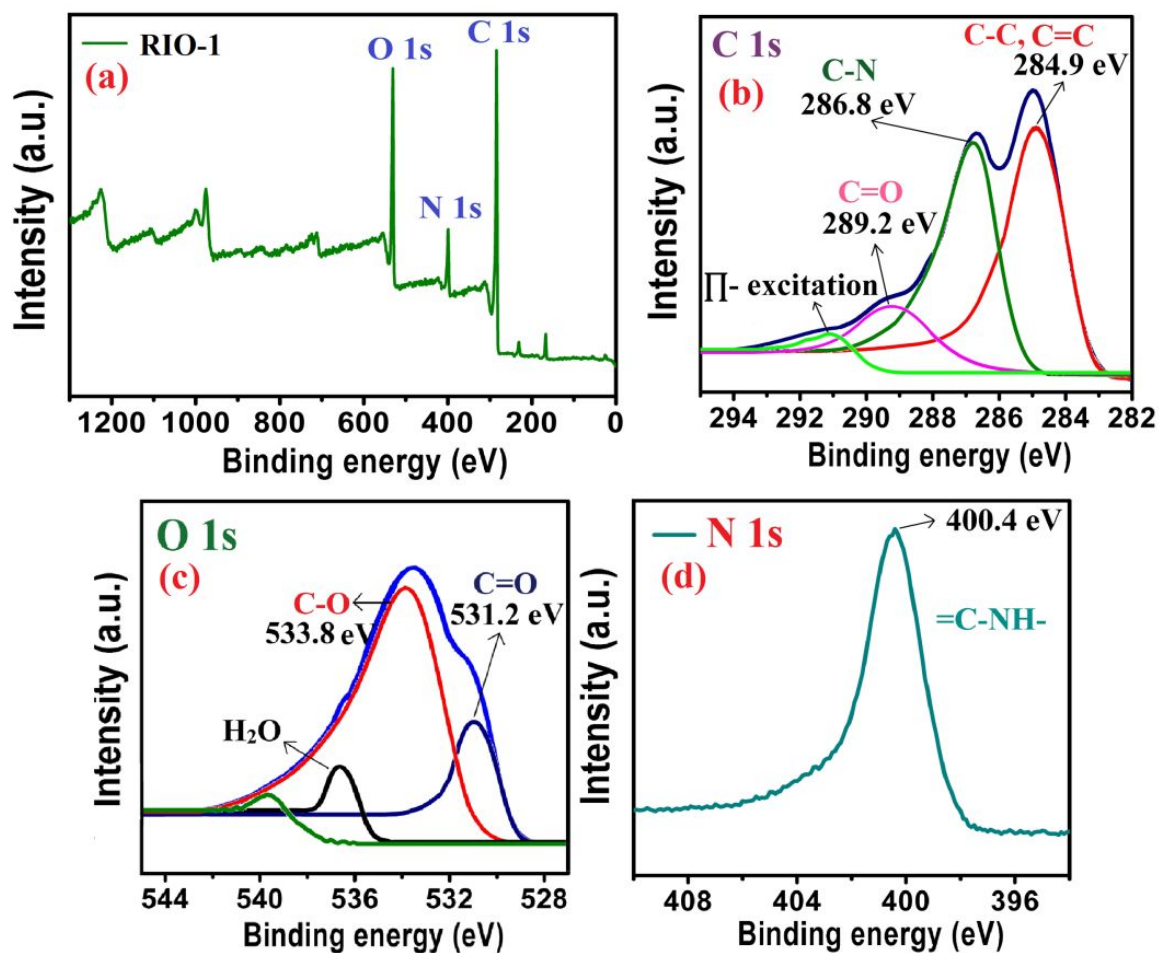**Figure S7:** FT-IR spectrum of reused Zn@RIO-1.

Figure S8. XPS survey scan measurement on RIO-1 material (a), C1s narrow scan (b), O1s narrow scan measurement (c) and N1s narrow scan (d) on the parent COF (RIO-1).

Table S1. Effect of different parameters on the catalytic production of α-alkylidene cyclic carbonate[a]

Entry	Catalyst (mg)	Base (mmol)	Time (h)	GC yield of product (%)
1	-	DBU (5)	8	none
2	Zn@RIO-1 (10)	DBU (5)	8	78

3	ZnCl₂ (10)	DBU (5)	8	36
4	Zn(NO₃)₂ (10)	DBU (5)	8	21
5	Zn(OAc)₂.2H₂O (10)	DBU (5)	8	48
6	Zn@RIO-1 (10)	TBD (5)	8	66
7	Zn@RIO-1 (10)	DIPEA (5)	8	54
8	Zn@RIO-1 (10)	DABCO (5)	8	52
9	Zn@RIO-1 (10)	NEt₃ (5)	8	48
10	Zn@RIO-1 (10)	t-BuOK (5)	8	68
11	Zn@RIO-1 (10)	K₂CO₃ (5)	8	42
12	Zn@RIO-1 (10)	Cs₂CO₃ (5)	8	49
13	Zn@RIO-1 (5)	DBU (5)	8	56
14	Zn@RIO-1 (15)	DBU (5)	8	89
15	Zn@RIO-1 (20)	DBU (5)	8	89
16	Zn@RIO-1 (15)	DBU (5)	10	100
17	Zn@RIO-1 (15)	DBU (4)	10	78
18	Zn@RIO-1 (15)	DBU (6)	10	100
19	RIO-1 (15)	DBU (5)	10	53

[a]*Reaction condition: 2-methylbut-3-yn-2-ol (5 mmol), CO₂ (1 atm), Base (5 mmol), room temperature, no solvent.*
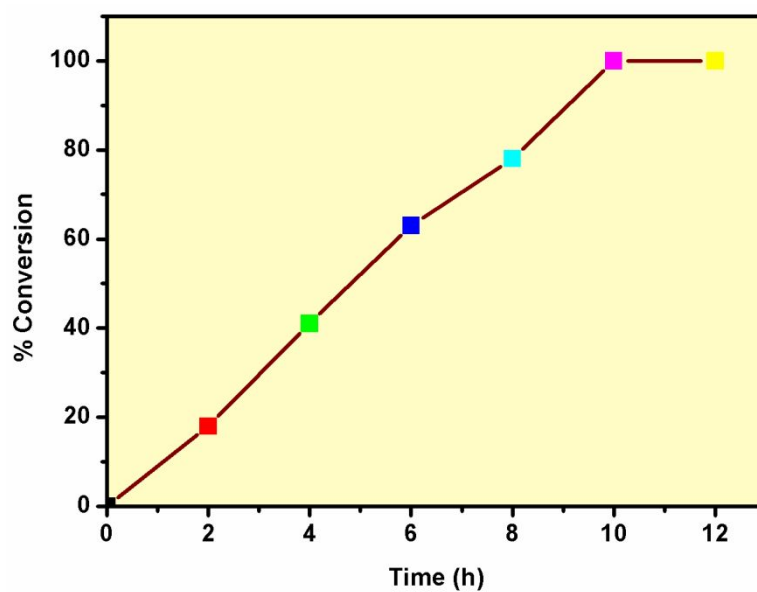
Figure S9. Kinetic plot of catalytic α-alkylidene cyclic carbonate formation reaction [reaction conditions: 2-methylbut-3-yn-2-ol (5 mmol), DBU (5 mmol), CO_2 (1 atm), room temperature, no solvent].

Table S2. Effect of different parameters on the catalytic synthesis of 2-oxazolidinones from 2-methyl-3-butynol and benzylamine via CO_2 fixation[a]

Entry	Catalyst (mg)	Time (h)	Temperature (°C)	Yield of product (%)[b]
1	-	12	RT	0
2	Zn@RIO-1 (15)	12	RT	45
3	Zn@RIO-1 (15)	12	50	62
4	Zn@RIO-1 (15)	12	60	77

5	Zn@RIO-1 (15)	12	70	86
6	Zn@RIO-1 (15)	12	80	94
7	Zn@RIO-1 (15)	12	90	88
8	Zn@RIO-1 (10)	12	80	76
9	Zn@RIO-1 (20)	12	80	94
10	RIO-1 (15)	12	80	38
11	$ZnCl_2$ (10)	12	80	34

**a*Reaction condition*: *2-methyl-3-butynol (5 mmol)*, benzylamine *(5 mmol)*, CO_2 *(1 atm)*, *No solvent;* [b]*isolated yield.*
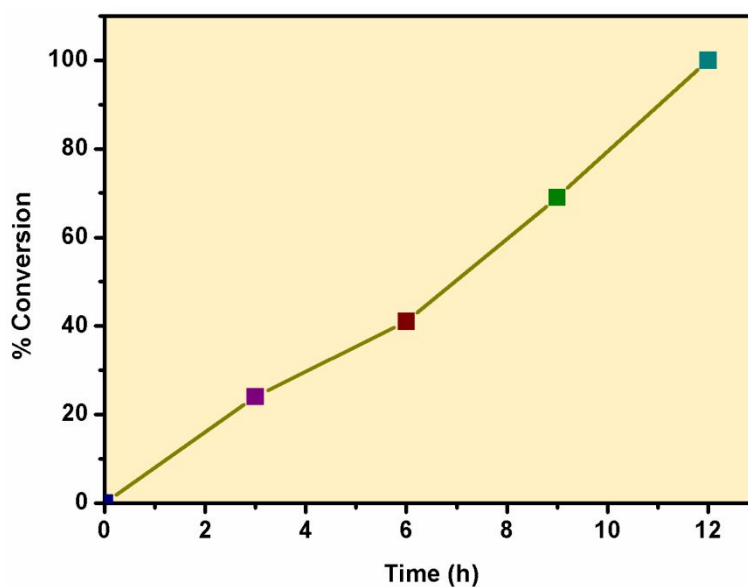
Figure S10. Kinetic plot of catalytic synthesis of 2-oxazolidinones from 2-methyl-3-butynol and benzylamine *via* carbon dioxide fixation reaction [Reaction conditions: 2-methylbut-3-yn-2-ol (5 mmol), benzylamine (5 mmol), CO_2 (1 atm), No solvent].

Table S3. Comparison table for the catalytic syntheses α-alkylidene cyclic carbonate and oxazolidinones from propargylic alcohol via carbon dioxide fixation reactions between this works with previous reports

Reaction	Catalyst	Reaction conditions	Catalytic nature	Yield (%)[a]	Ref.
α-alkylidene cyclic carbonate	ZnI$_2$/ NEt$_3$	2-methylbut-3-yn-2-ol (1.5 mmol), NEt$_3$ (1.5 mmol), ZnI$_2$ (0.3 mmol), 1 MPa CO$_2$, 30°C, 14h	Homogeneous	95	18
	AgOAc	2-methylbut-3-yn-2-ol (5 mmol), AgOAc (1 mol%), DavePhos (2 mol %), CO$_2$ (20 bar), CH$_3$CN (10 mL), rt, 16h	Homogeneous	87	16
	(nBu$_4$N)$_2$O$_x$	2-methylbut-3-yn-2-ol (0.03 mmol), (nBu$_4$N)$_2$O$_x$ (2.5 mol%), CO$_2$ (80 bar), 80°C, 24h	Homogeneous	100 (99)[b]	21
	Ag@RB-POP	2-methylbut-3-yn-2-ol (0.5 mmol), Ag@RB-POP (20 mg, 0.01 mol% Ag based	Heterogeneous	87	15

		on 1); DBU (0.5 mmol), CO$_2$ (1 MPa), CH$_3$CN (2 mL), 30°C, 12 h			
	Zn@BBAPA-1	2-methylbut-3-yn-2-ol (1.5 mmol), DBU (1.5 mmol), Zn@BBAPA-1 (50 mg), CO$_2$ (1 MPa), 30°C, 6h	Heterogeneous	98	24
	Zn@RIO-1	2-methylbut-3-yn-2-ol (5 mmol), DBU (5 mmol), CO$_2$ (1 atm), Zn@RIO-1 (15 mg), CO$_2$ (1 atm), room temperature, 10h	Heterogeneous	96	This report
Oxazolidinones	Ag$_2$WO$_4$/Ph$_3$P	2-methylbut-3-yn-2-ol (5 mmol), cyclohexylamine (5 mmol), Ag$_2$WO$_4$ (23.2 mg, 1 mol%), Ph$_3$P (26.2 mg, 2 mol%), CO$_2$ (0.5 MPa), 50°C, 12h	Homogeneous	85	36
	Ag$_2$CO$_3$	1st step reaction: 2-methylbut-3-yn-2-ol (100 mmol), Ag$_2$CO$_3$ (2.8 mg, 0.01 mol%), (p-MeOC$_6$H$_4$)$_3$P (14.1 mg,	Homogeneous	92.5[c]	37

		0.04 mol%), CO_2 (2.0 MPa), $CHCl_3$ (2 mL), 25˚C, 96h; 2nd step reaction cyclohexylamine (100 mmol), 10 mL $PhCH_3$ and 2.0 g 4Å MS at 120˚C for 2 h			
	CuI/[P$_{4444}$][Im]	2-methylbut-3-yn-2-ol (1 mmol), cyclohexylamine (1 mmol), CuI/[P$_{4444}$][Im] (0.1 mmol), CO_2 (1 atm), 30˚C, 24h	Homogeneous	82	38
	Zn@RIO-1	2-methylbut-3-yn-2-ol (5 mmol), cyclohexylamine (5 mmol), Zn@RIO-1 catalyst (15 mg), CO_2 (1 atm), 80˚C, 10h	Heterogeneous	92	This report

^{a}Isolated yield; ^{b}%Conversion (% selectivity); ^{c}Determined by GC with biphenyl as the internal standard.
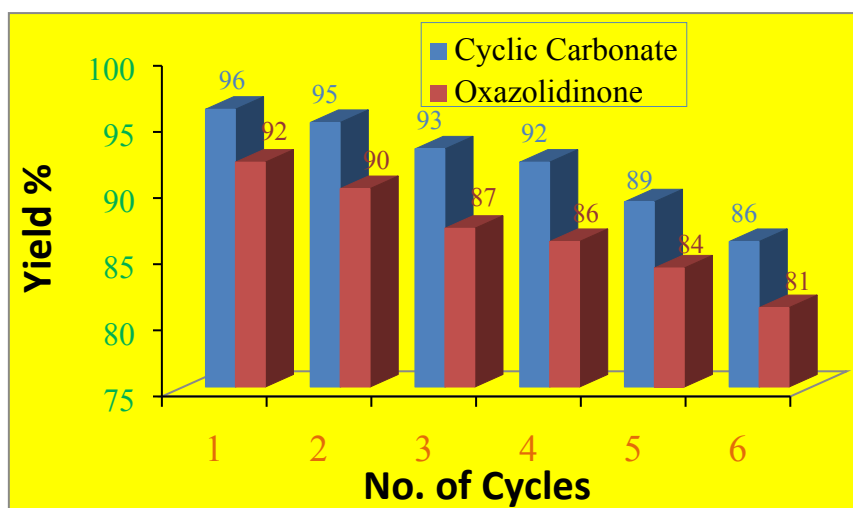
Figure S11. Heterogeneity cycle of Zn@RIO-1 catalyst for the catalytic synthesis of α-alkylidene cyclic carbonates and oxazolidinones from propargylic alcohols.

PXRD patterns and IR Spectra demonstrate outstanding chemical stability to boiling water, aqueous acid (6 N HCl) or 6N H_2SO_4 and base (6 N NaOH). As seen from PXRD patterns and FTIR spectra, there is no noticeable change between newly synthesized catalyst and the catalyst after treatment with hot water, 6N NaOH, 6N HCl and 6N H_2SO_4.
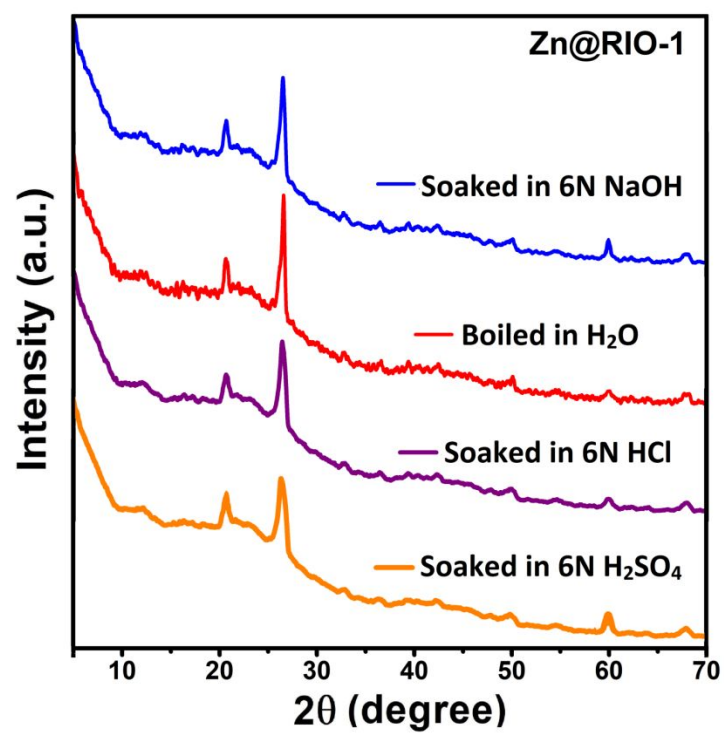
Figure S12. Chemical stability demonstrated from XRD patterns.
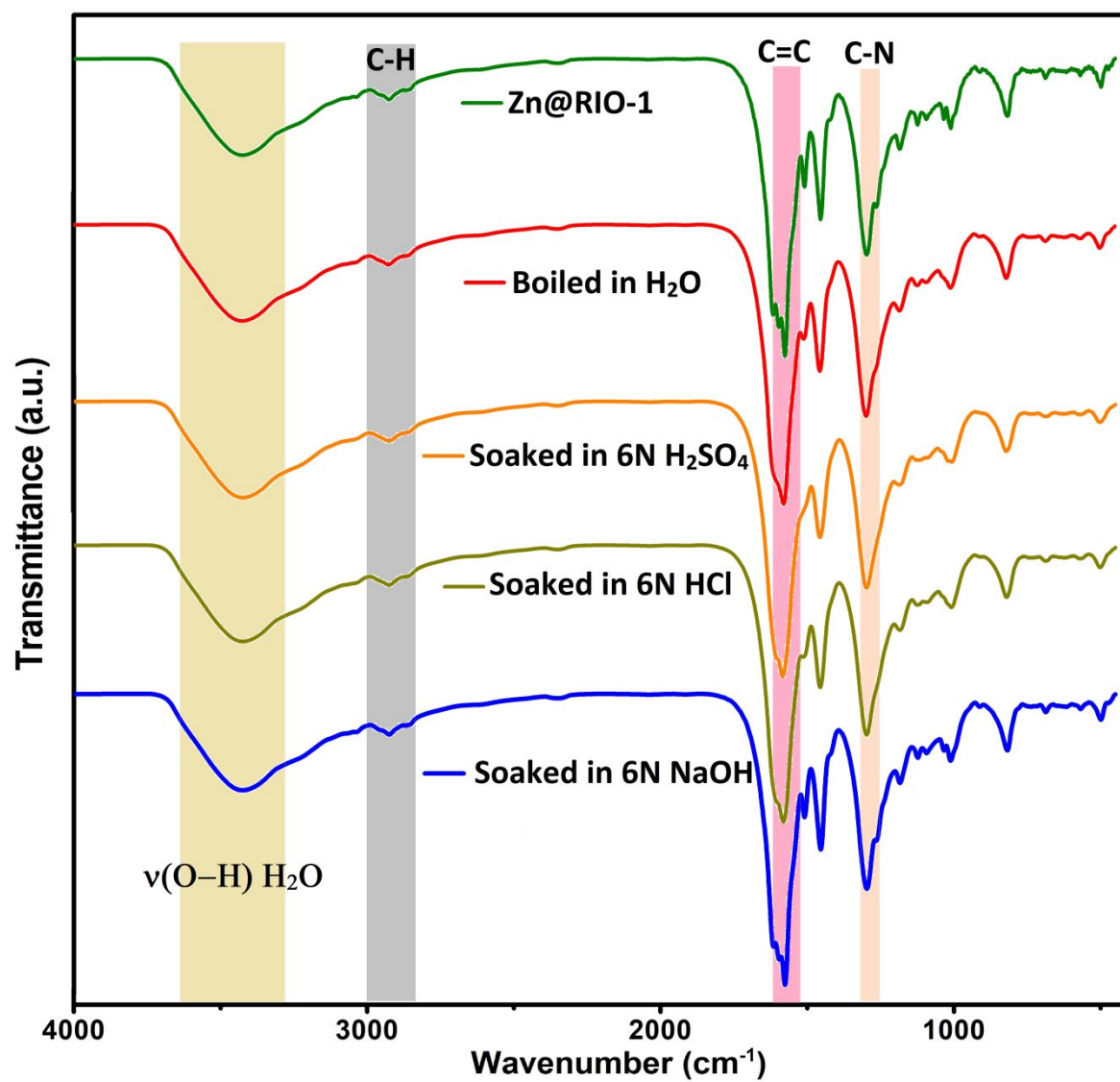
Figure S13. Chemical stability demonstrated from IR spectra.

Powder Refinement: Rwp = 7.87%   Rwp(w/o bck) = 69.03% Rp = 6.15%
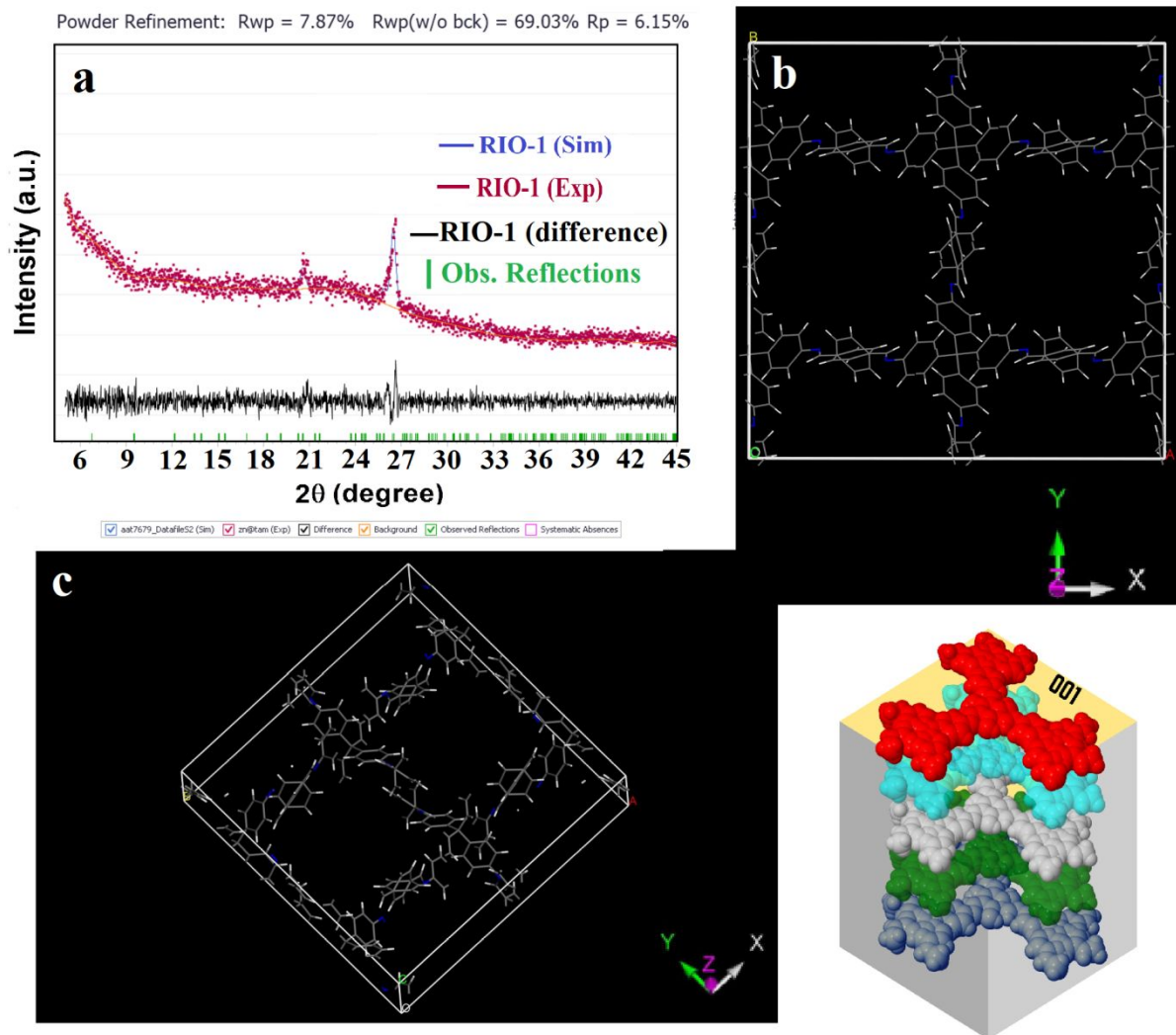
Figure S14: (a) Experimental (deep pink) compared with Pawley refined (blue) PXRD profiles of 3D COF-**RIO-1**; difference plot is given in black colour. (b,c) The lattice model was simulated using BIOVIA Material Studio 2017
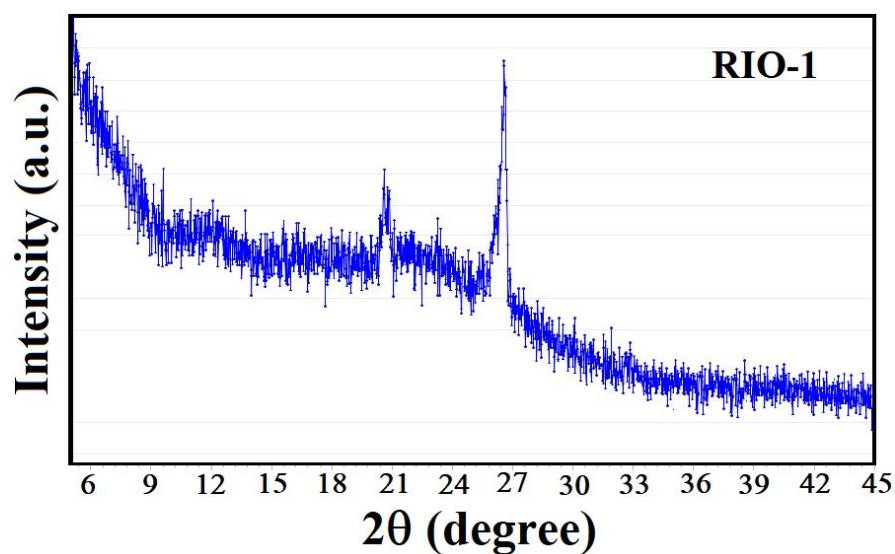
Figure S15. Powder X-ray diffraction pattern of 3D COF (RIO-1) material.
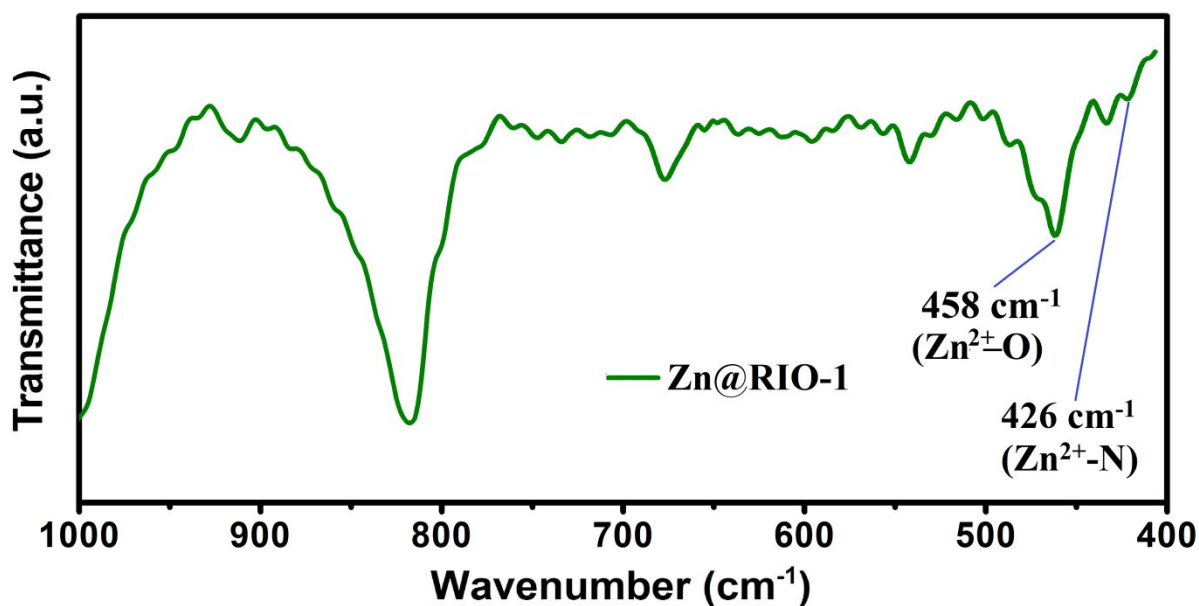
Figure S16. Zoom-in FTIR spectrum of Zn@RIO-1, showing Zn^{2+}-O and Zn^{2+}-N coordination.

Zoom-in FTIR spectrum of Zn@RIO-1 (Fig. S16) clearly shows that Zn^{2+} is coordinated to 3D COF through N and O. The sharp peak positioned at 458 cm^{-1} is attributed to the Zn-O stretching bonds. The band located at 426 cm^{-1} is ascribed to the Zn-N stretching frequencies in Zn@RIO-1.
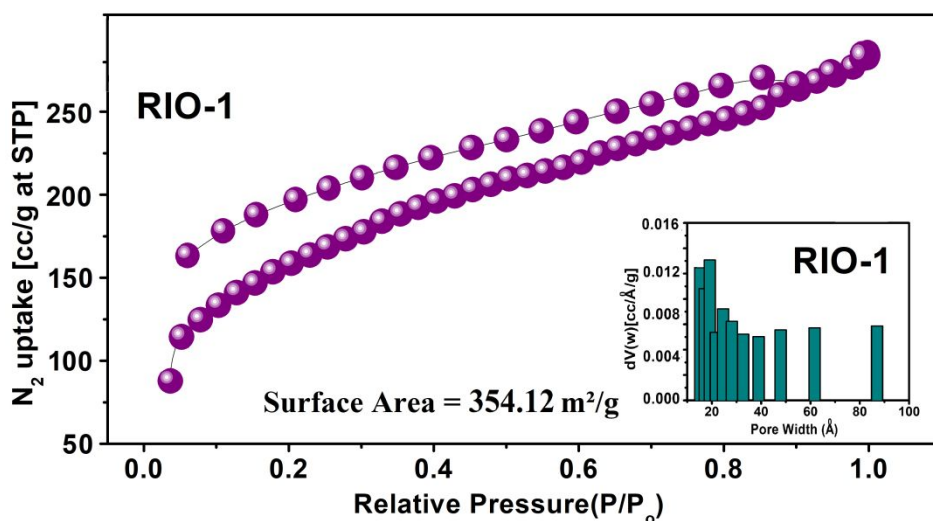
Figure S17. N_2 adsorption–desorption isotherm of RIO-1 material at a certain temperature (77 K). Pore size distribution is shown in the inset.
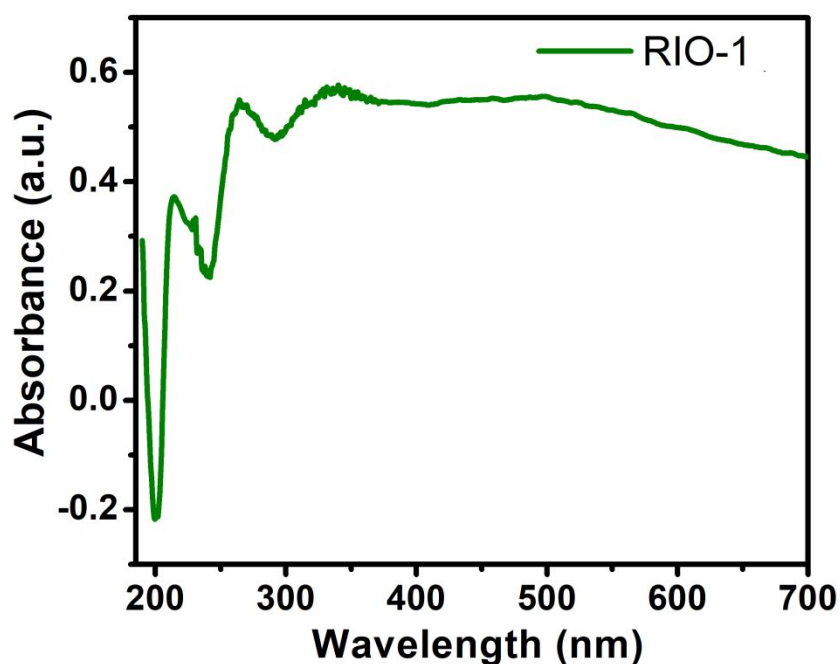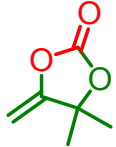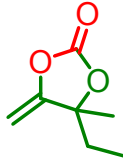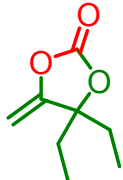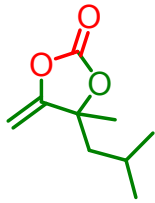
Figure S18. UV-vis spectrum of 3D COF (RIO-1).

Characterizations data of respective *α*-alkylidene cyclic carbonates[5]

[4,4-dimethyl-5-methylene-1,3-dioxolan-2-one]: ^{1}H NMR (400 MHz, CDCl$_3$): δ (in ppm) 1.594 (s, 6H), 4.297 (d, J = 4.0, 1H), 4.723 (d, J = 4.0, 1H).	
[4-ethyl-4-methyl-5-methylene-1,3-dioxolan-2-one]: ^{1}H NMR (400 MHz, CDCl$_3$): δ (in ppm) 1.010 (t, J = 7.6, 3H), 1.507 (s, 3H), 1.755 (d, J = 7.2, 2H), 4.324 (d, J = 4.2 Hz, 1H), 4.708 (d, J = 4.2 Hz, 1H).	
[4,4-diethyl-5-methylene-1,3-dioxolan-2-one]: ^{1}H NMR (400 MHz, CDCl3): δ (in ppm) 0.981 (t, J = 7.4 Hz, 6H), 1.503-1.6021 (m, 2H), 1.791-1.892 (m, 2H), 4.322 (d, J = 4.4 Hz, 2H), 4.701 (d, J = 4.2 Hz, 2H).	
[4-isobutyl-4-methyl-5-methylene-1,3-dioxolan-2-one]: ^{1}H NMR (400 MHz, CDCl3): δ (in ppm) 1.083 (t, J = 7.6 Hz, 6H), 1.575 (s, 3H), 1.969-2.152 (m, 2H), 4.313 (d, J = 4.0 Hz, 2H), 4.709 (d, J = 4.2 Hz, 2H).	

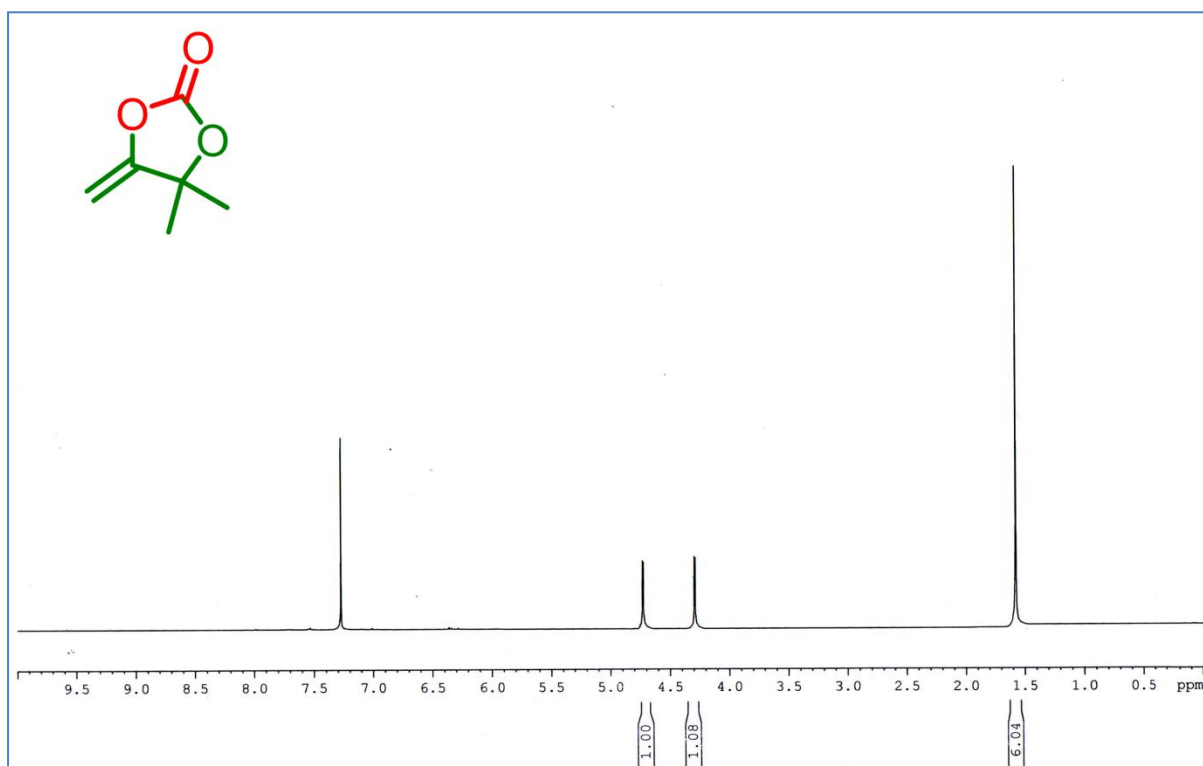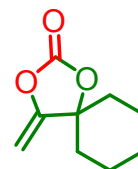| **[4-methylene-1,3-dioxaspiro[4.5]decan-2-one]:** ^{1}H NMR (400 MHz, CDCl3): δ (in ppm) 1.135-1.228 (m, 1H), 1.423-1.587 (m, 5H), 1.598-1.694 (m, 2H), 1.808-1.892 (m, 2H), 4.286 (d, *J* = 4.2 Hz, 2H), 4.753 (d, *J* = 4.2 Hz, 2H).	

Figure S19: ^{1}H NMR of 4,4-dimethyl-5-methylene-1,3-dioxolan-2-one.
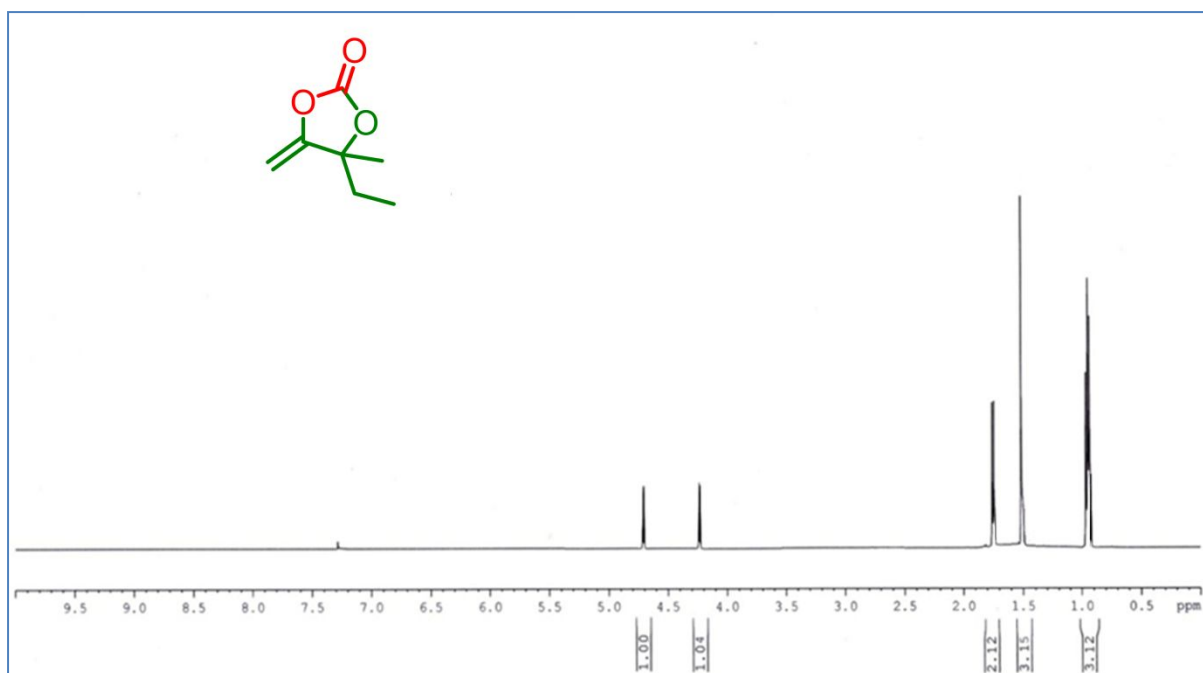
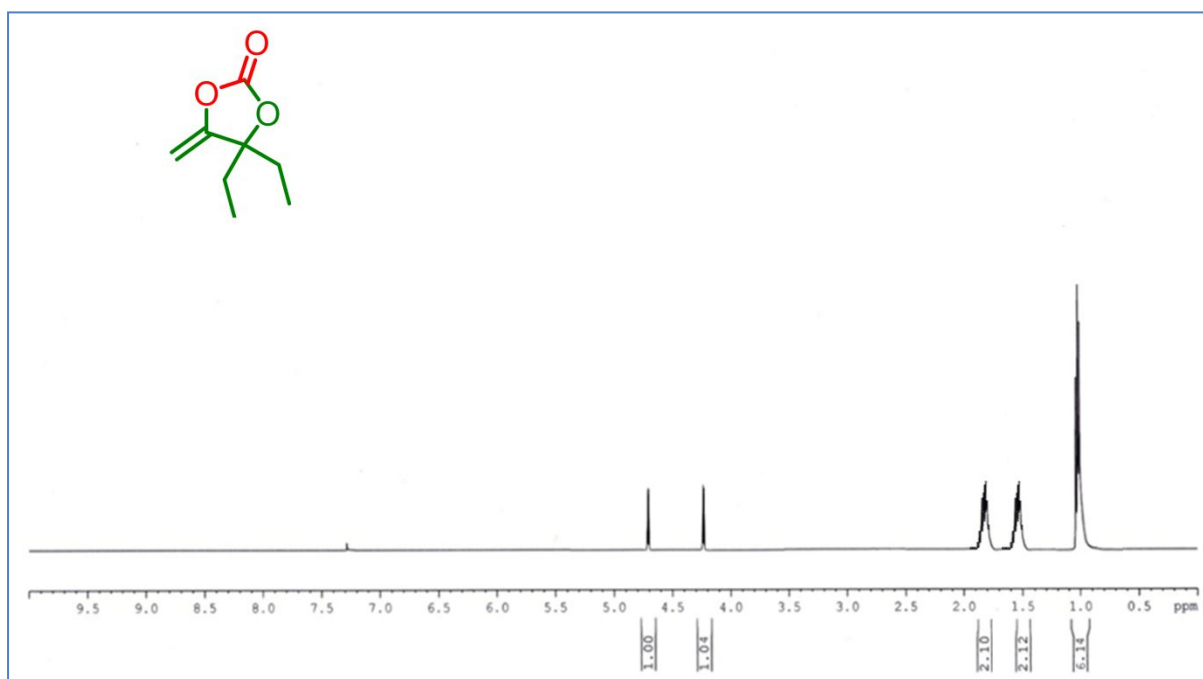**Figure S20:** ^{1}H NMR of 4-ethyl-4-methyl-5-methylene-1,3-dioxolan-2-one.

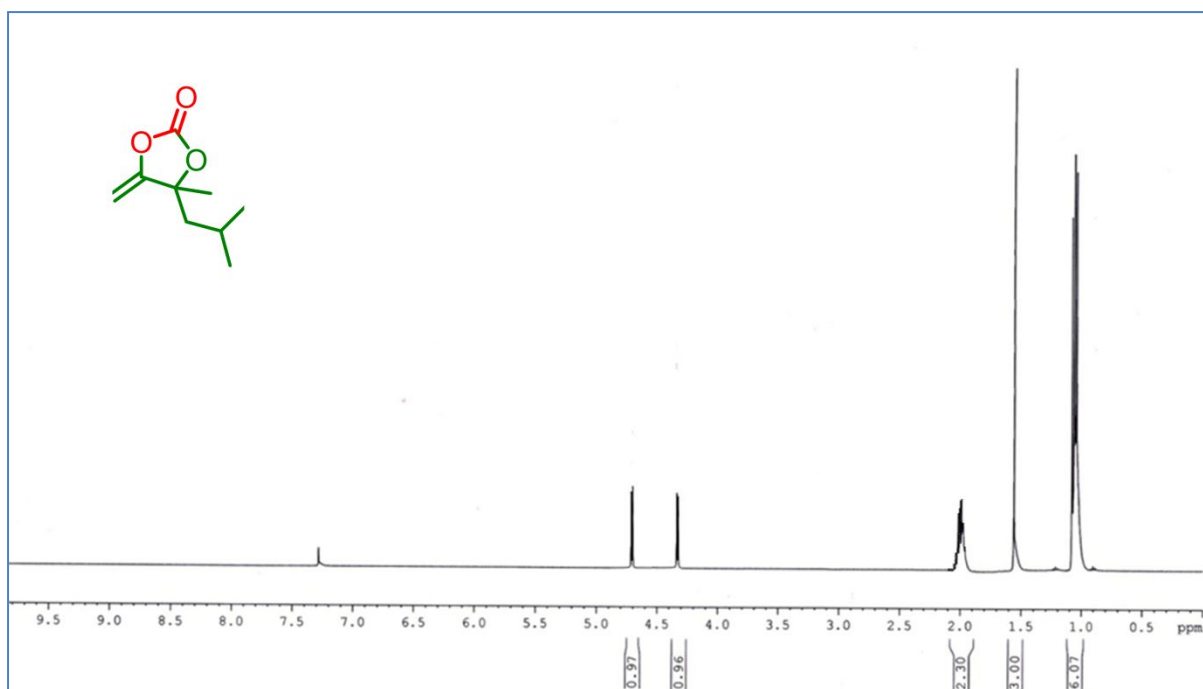**Figure S21:** ^{1}H NMR of 4,4-diethyl-5-methylene-1,3-dioxolan-2-one.

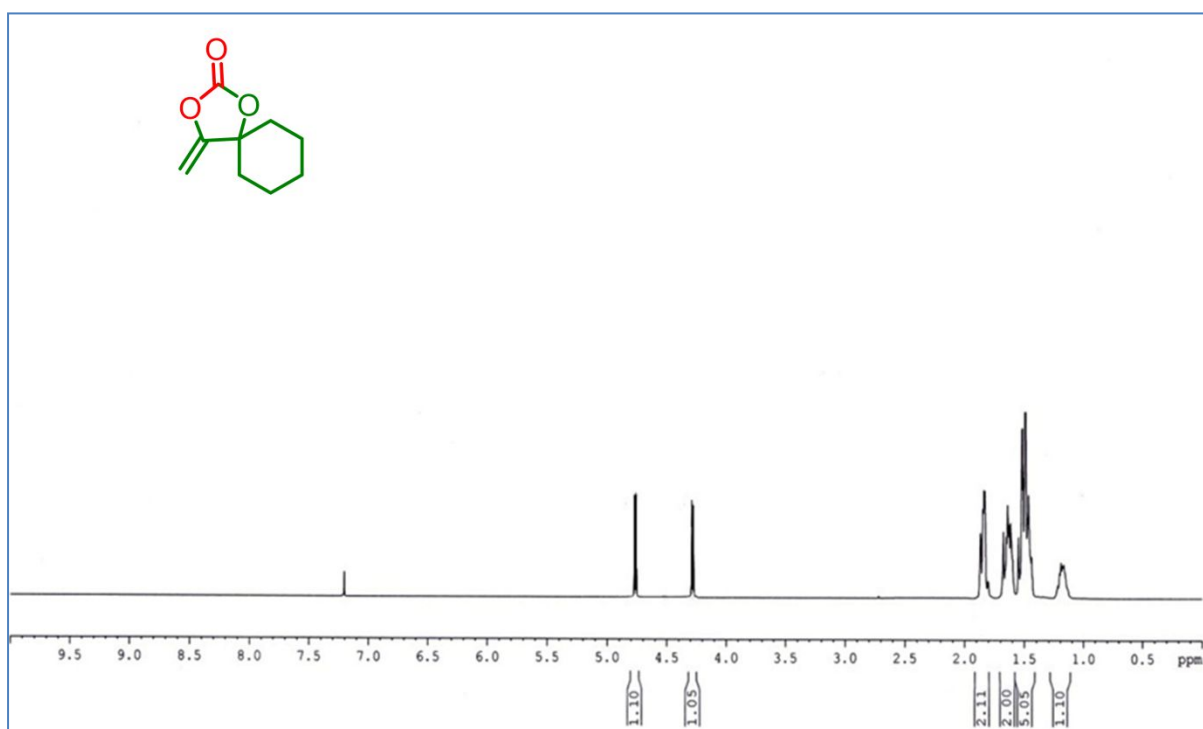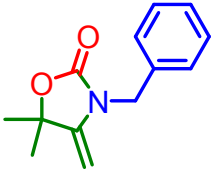**Figure S22:** ^{1}H NMR of 4-isobutyl-4-methyl-5-methylene-1,3-dioxolan-2-one.
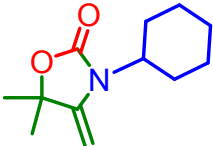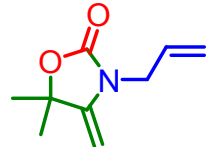

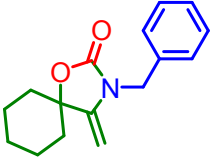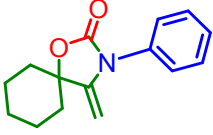**Figure S23:** ^{1}H NMR of 4-methylene-1,3-dioxaspiro[4.5]decan-2-one.

Characterizations data of respective 2-oxazolidinones[6]

|	
[3-Benzyl-5,5-dimethyl-4-methylene-oxazolidin-2-one]: ^{1}H NMR (CDCl$_3$, 400 MHz) δ 7.42-7.25 (m, 5H, Ar-H), 4.66 (s, 2H), 4.04 (d, J = 4.0 Hz, 1H), 3.95 (d, J = 2.4 Hz, 1H), 1.52 (s, 6H) ppm.	
[3-Cyclohexyl-5,5-dimethyl-4-methylene-oxazolidin-2-one]: ^{1}H NMR (CDCl$_3$, 400 MHz) δ 4.12 (d, J = 4.0 Hz, 1H), 3.96 (d, J = 4.0 Hz, 1H), 3.53 (t, J = 8.0 Hz, 2H), 1.86-1.14 (13H) ppm.	
[3-Allyl-5,5-dimethyl-4-methylene-oxazolidin-2-one]: ^{1}H NMR (CDCl$_3$, 400 MHz) δ 5.82-5.92 (m, 1H), 5.19-5.31 (s, 2H), 4.62-69 (m, 2H), 4.06-4.11 (m, 2H), 1.52 (s, 6H) ppm.	
[3-Benzyl-4-methylene-1-oxa-3-aza-spiro[4.5]decan-2-one]: ^{1}H NMR (CDCl$_3$, 400 MHz) δ 7.41-7.23 (m, 5H, Ar-H), 4.62 (s, 2H), 4.07 (d, J = 3.9 Hz, 1H), 3.98 (d, J = 2.3 Hz, 1H), 1.21-1.90 (m, 10H) ppm.	
[4-methylene-3-phenyl-1-oxa-3-azaspiro[4.5]decan-2-one]: ^{1}H NMR (CDCl$_3$, 400 MHz) δ 7.51-7.93 (m, 5H, Ar-H), 4.29 (dd, J = 2.4, 9.0 Hz, 1H), 0.95-1.79 (m, 10H) ppm.	
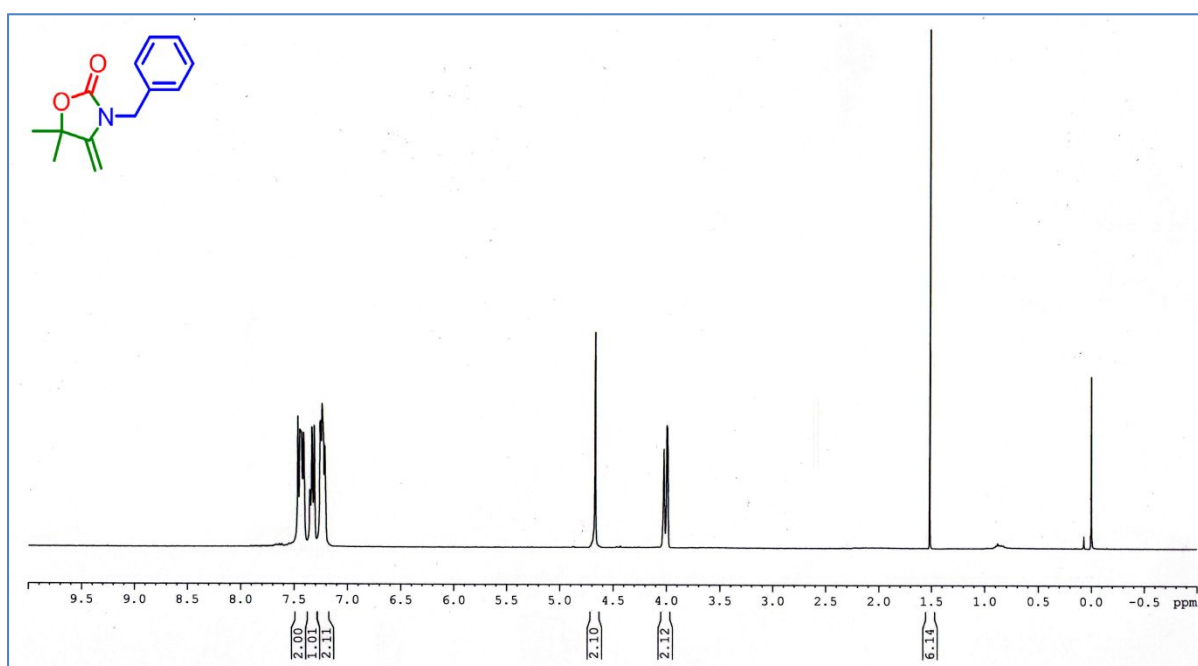
Figure S24: ^{1}H NMR of 3-Benzyl-5,5-dimethyl-4-methylene-oxazolidin-2-one.
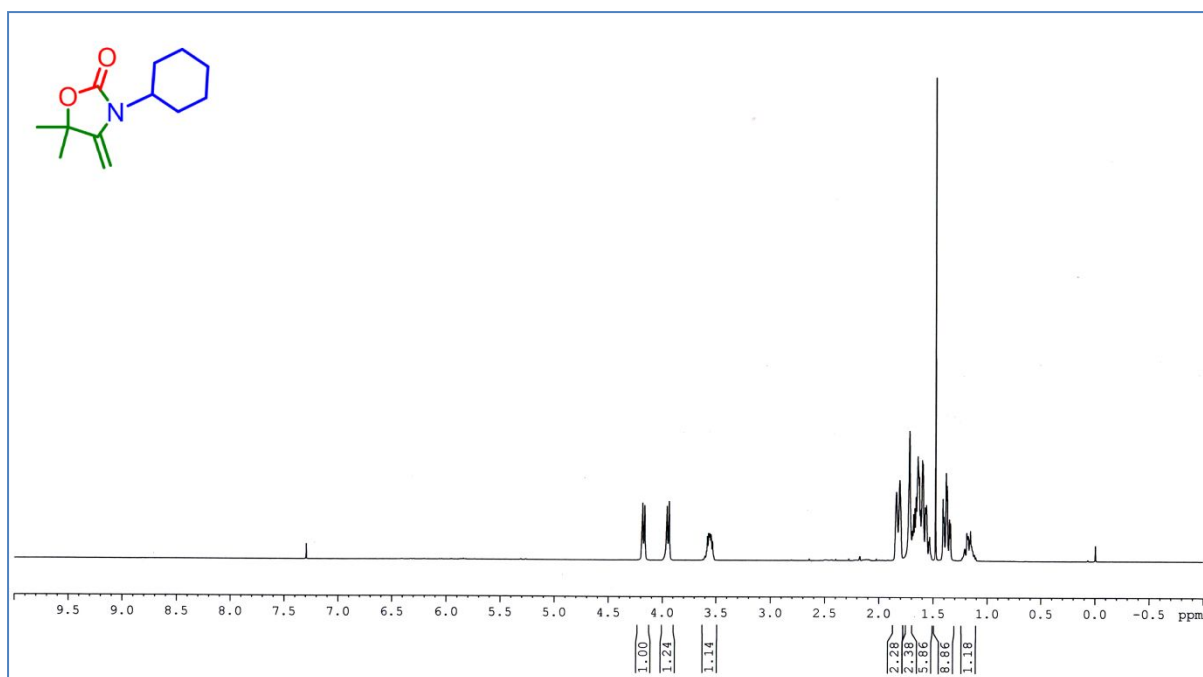
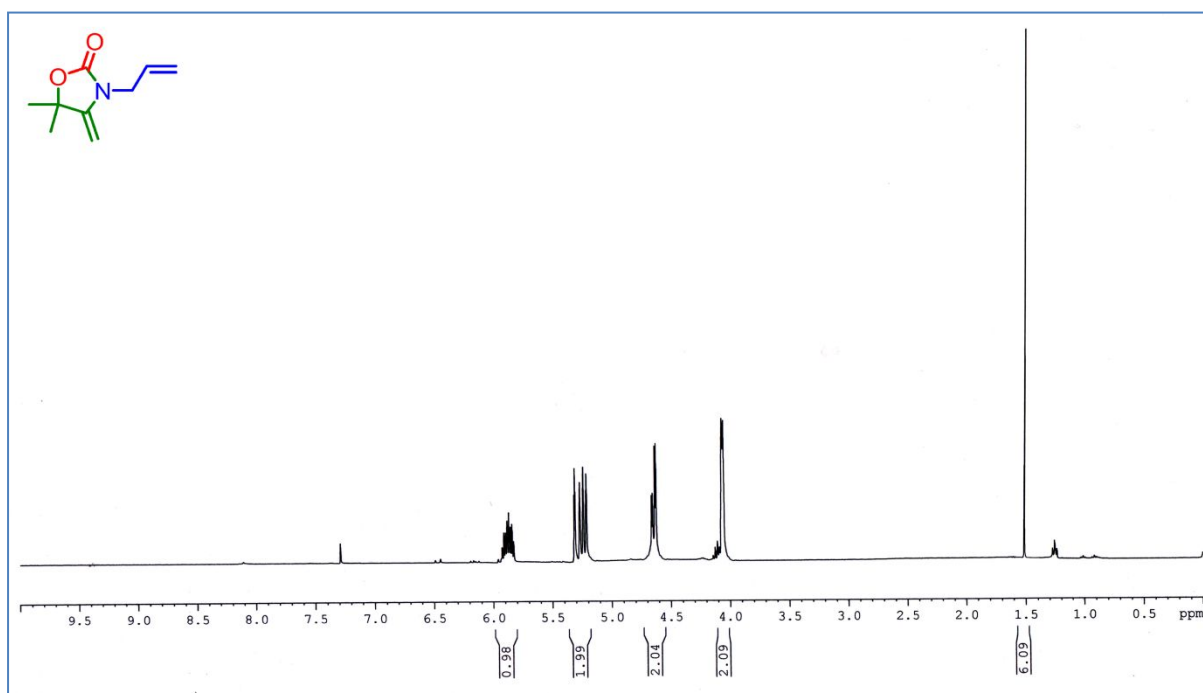**Figure S25:** ¹H NMR of 3-Cyclohexyl-5,5-dimethyl-4-methylene-oxazolidin-2-one.

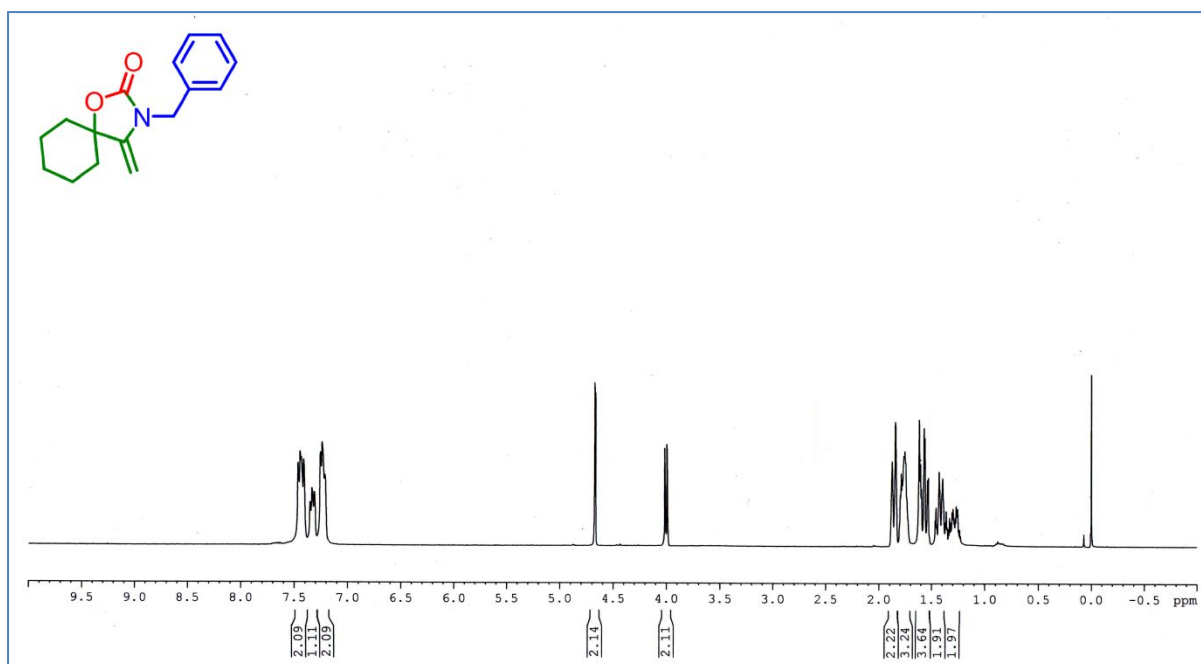**Figure S26:** ¹H NMR of 3-Allyl-5,5-dimethyl-4-methylene-oxazolidin-2-one.

Figure S27: ^{1}H NMR of 3-Benzyl-4-methylene-1-oxa-3-aza-spiro[4.5]decan-2-one.
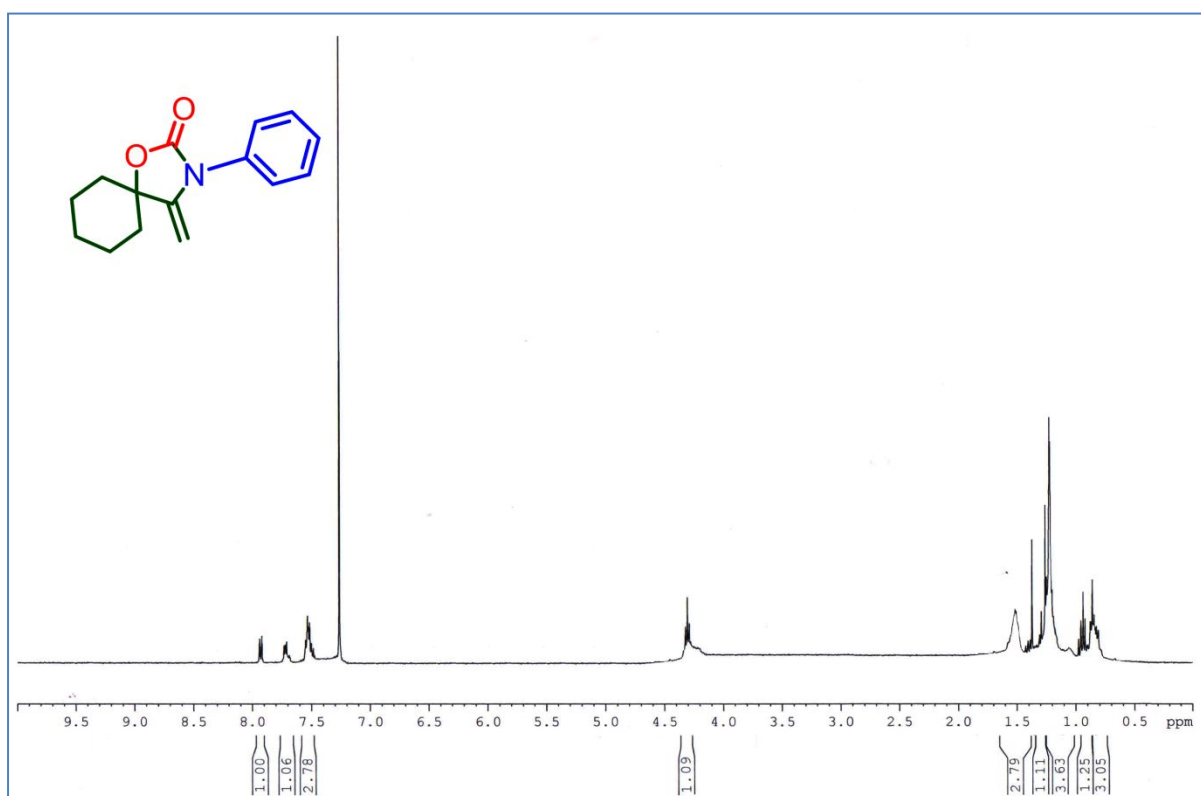

Figure S28: ^{1}H NMR of 4-methylene-3-phenyl-1-oxa-3-azaspiro[4.5]decan-2-one.

References:

(1) Yelamaggad, C. V.; Achalkumar, A. S.; Shankar Rao, D. S.; Prasad, S.K.; Luminescent, Liquid Crystalline Tris(*N*-salicylideneaniline)s: Synthesis and Characterization, *J. Org. Chem*. **2009**, *74*, 3168-3171.

(2) Kandambeth, S.; Mallick, A.; Lukose, B.; Mane, V. M.; Heine, T.; Banerjee, R.; Construction of Crystalline 2D Covalent Organic Frameworks with Remarkable Chemical (Acid/Base) Stability via a Combined Reversible and Irreversible Route, *J. Am. Chem.Soc*. **2012**, *134*, 19524-19527.

(3) Islam, S. S.; Biswas, S.; Molla, R. A.; Yasmin, N.; Sk. Islam, S. M.; Green Synthesized AgNPs Embedded in COF: An Efficient Catalyst for the Synthesis of 2-Oxazolidinones and α-Alkylidene Cyclic Carbonates via CO_2 Fixation, *ChemaNanoMat*, **2020**, 6, 9, 1386-1397.

(4) Li, W., Ren, P., Zhou, Y., Feng, J., & Ma, Z. (2019). Europium(III) functionalized 3D covalent organic framework for quinones adsorption and sensing investigation, *Journal of Hazardous Materials*, **2019**, 121740.

(5) Wu, Z.; Lan, X.; Zhang, Y.; Lia M.; and Bai, G.; Copper(i) iodide cluster-based lanthanide organic frameworks: synthesis and application as efficient catalysts for carboxylative cyclization of propargyl alcohols with CO_2 under mild conditions, *Dalton Trans*. **2019**, *48*, 11063-11069.

(6) Ghosh, S.; Riyajuddin, S.; Sarkar, S.; Ghosh, K.; Islam, S. M.; Pd NPs Decorated on POPs as Recyclable Catalysts for the Synthesis of 2–Oxazolidinones from Propargylic Amines via Atmospheric Cyclizative CO_2 Incorporation, *ChemNanoMat*, **2020**, *6*, 160-172.